Technical Report PUR-30-P

PROJECT SQUID

A COOPERATIVE PROGRAM
OF FUNDAMENTAL RESEARCH
AS RELATED TO JET PROPULSION
FOR THE
OFFICE OF NAVAL RESEARCH, DEPARTMENT OF THE NAVY
OFFICE OF SCIENTIFIC RESEARCH, DEPARTMENT OF THE AIR FORCE
AND THE
OFFICE OF ORDNANCE RESEARCH, DEPARTMENT OF THE ARMY

Contract N6-ori-105, Task Order III, NR-098-038

THE STRUCTURE OF OXIDE SCALES ON CHROMIUM STEELS

by

H. J. Kearian, E. C. Randell and T. A. Longo

Purdue University
Lafayette, Indiana

February 1957

PROJECT SQUID HEADQUARTERS
JAMES FORRESTAL RESEARCH CENTER
PRINCETON UNIVERSITY
PRINCETON, N. J.

The Structure of Oxide Scales on Chromium Steels*

By H. J. YEARIAN,* E. C. RANDELL* and T. A. LONGO*

Abstract

The structure of the oxide scale formed on commercial chromium steels containing 5 to 26 percent Cr when oxidized in air or oxygen at temperatures from 700 C to 1160 C for times up to 100 hours were determined by X-ray diffraction methods, supplemented in some instances by chemical analysis. Two distinct types of scale were observed: A type scale occurs when the rate of metal loss is less than approximately 10 mg/cm²/day, and B type when the attack rate is in the excessive range. For exposures near the critical conditions an initial A type scale transforms to B type during oxidation.

The essential component of A type scale is Cr_2O_3. This is usually accompanied by αFe_2O_3 in an amount which increases with the iron content of the alloy (i.e., with rate of attack). At high temperatures or long oxidation times, dilute solid solutions of each of these phases in the other are formed. When the alloy contains a few tenths percent of Mn, the A type scale may also include copious amounts of $MnCr_2O_4$, especially for high chrome alloys and for low temperature oxidations in air.

B type scale is more complex than A scale and may be considered as two layers. The outer layer is duplex and is similar in all respects to the Fe_3O_4 and Fe_2O_3 layers of the scale on pure iron. The major constituent of the inner layer, corresponding to the FeO layer on pure iron, is a solid solution, $FeFe_{2-x}Cr_xO_4$, of the spinel type. Throughout most of the layer x varies slowly, but near the metal it rises rapidly to $x = 2$ and near the Fe_3O_4 layer it falls rapidly to $x = 0$. The mean value of x lies in the range of about 0.5 to 1.5. The greater the chromium content of the alloy, the higher the temperature and the longer the time of oxidation, the larger is the value of x. In cases of very high attack the series of spinels is accompanied by a series of wustites which are modified by chromium additions ranging downward to zero at the Fe_3O_4 layer. For 10 to 20 hour oxidations at 925 C and at 1000 C the chromium fraction of total metal in the inner layer is about 1.8 times its value in the alloy, whereas the excess is only about one percent in the scale as a whole.

The experimental data are compared and contrasted with existing information and are qualitatively interpreted by use of a tentatively proposed Fe-Cr-O phase diagram and a special theory of alloy oxidation. 3.2.3

Introduction

MANY INVESTIGATIONS have been made of the protective oxides formed on heat resistant alloys at high temperatures. The problem is so complex, however, that even for the simplest of these alloys no complete picture of the oxide scale structure can be drawn for a wide variety of alloy compositions and exposure conditions. Most of the information now available is restricted to conditions giving rise to relatively high attack rates.

It was the intent of the present research to obtain a sufficiently detailed description of the scale structure in the case of the simple chromium steels that the essential correlations between oxide type and attack rate could be determined. Establishment of such correlation was the first step toward an understanding of the oxidation mechanism. The primary means of identification of the oxide phases present and their relative amounts was use of one or more of the standard X-ray diffraction techniques. In certain instances these interpretations were supplemented by chemical analysis. Similar investigations regarding the nickel-chromium steels have been made and will be presented in the near future.

Because of the unavailability of pure binary alloys having a range of composition sufficiently wide for the purpose, the major part of the work was carried out with commercial wrought sheet materials of nominal 5, 13, 17 and 26 percent chromium content. Their complete analyses are shown in Table 1. In view of the well established relationships between attack rate and chromium content of the commercial alloys[1] it was believed that the essential correlations with oxide type should be discernible independent of reasonable variations of the minor constituents. Certain aspects of the results were checked with a series of special alloys.

Experimental

Samples cut to approximately 1-inch x ¾-inch x 3/32-inch dimensions were polished through 3/0 emery papers and vapor degreased. For convenience in handling in the oxidizing furnace they were suspended from a Nichrome wire rack by platinum or Nichrome hooks. All oxide from the edges and the vicinity of the supports was excluded from the analysis.

Oxidation in air was carried out in a resistance furnace through which preheated dry air was passed at the rate of 200 cm³ per minute. The temperature was indicated by a thermocouple alongside the samples and was held constant to ±5° C. Treatments in oxygen were made in a quartz tube, the sealed end of which was inserted into the top of a furnace which was regulated to ±3° C by a Micromax controller. The open end of the quartz tube was waxed to a long water cooled brass tube fitted at its upper end with a packing gland and a sliding rod by means of which the samples could be lowered into the hot zone or withdrawn into the cold zone. The system was flushed twice by exhausting it to 0.01 mm of mercury and filling with dry oxygen. During oxidation the pressure was maintained slightly above one atmosphere.

Specimens for Debye-Scherrer X-ray diffraction analysis were made by powdering samples of the total scale or of separable layers obtained by flaking, scraping or controlled abrasion. This method was supplemented by Philips geiger counter spectrometer and back reflection investigations of the outer and inner surfaces of the scales or scale layers. The diffraction patterns were corrected for systematic errors caused by film shrinkage, specimen eccentricity and

★ Submitted for publication July 18, 1955.
* Physics Department, Purdue University, Lafayette, Indiana.

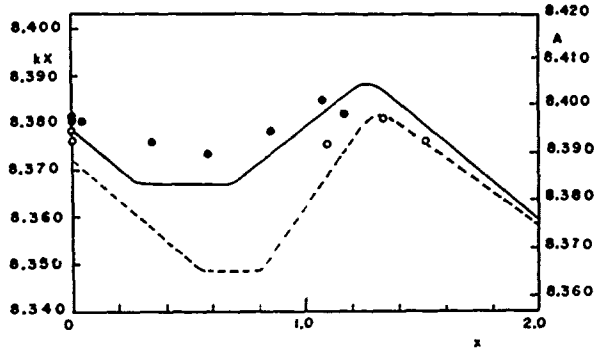

Figure 1—Lattice parameter of the $FeFe_{(2-x)}Cr_xO_4$ solid solution system measured at room temperature. Full curve, synthetic stoichiometric solutions quenched from 1180 C, 1100 C, 950 C; dashed curve, synthetic oxygen-rich solutions quenched from 950 C. From scale analysis: full circles, coexisting with wustite phases; open circles, without wustite.

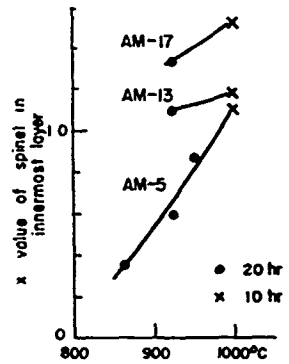

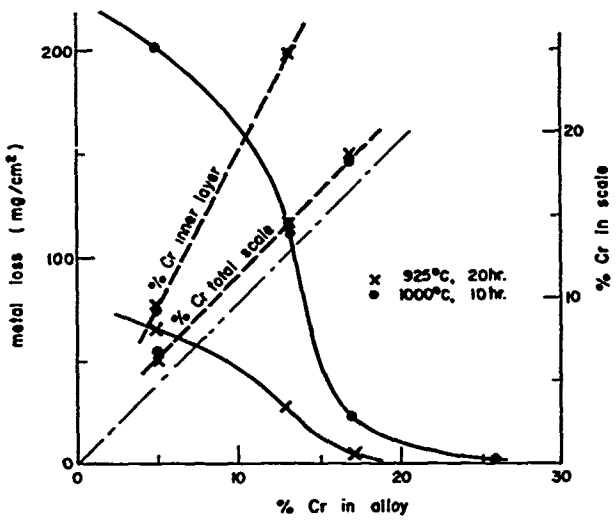

Figure 2—Metal loss of chromium steels and chromium content of B type scales. Full curves, metal loss; dashed curves, percent chromium metal in inner layer and in total scale. Small graph, variation with temperature of spinel x in innermost layer.

TABLE 1—Compositon of Alloys[1] (Weight Percent)

Sample	Cr	Ni	C	Mn	Si	P	S	N
AM-5	5.76	0.095	0.051	0.48	0.44	0.008	0.006	.....
AM-13	13.72	0.26	0.077	0.40	0.23	0.018	0.029	.....
AM-17	17.45	0.33	0.072	0.46	0.59	0.018	0.017	.....
AM-26	26.31	0.33	0.14	0.68	0.74	0.020	0.013	0.115

[1] Balance Fe.

absorption. From these diffraction patterns the oxide types present could be established from known interplanar spacing and lattice parameter data, and the mole fraction of the phases determined by comparison of the relative line intensities with those obtained from standard mixtures.

In the case of the Fe_2O_3—Cr_2O_3 solid solution system the lattice parameters given by Wretblad[2] were confirmed by new investigations. It was possible to determine the compositions to ±5 mole percent Cr_2O_3.

Because the spinel type oxides which are prevalent in the scales could not be completely identified from existing X-ray diffraction information, an intensive study[3] was made of synthetic Fe-Cr spinel oxide solutions, $FeFe_{(2-x)}Cr_xO_4$, $0 \leq x \leq 2$. This study revealed several interesting features regarding the cation arrangement in these oxides and the probable effect on their electrical conductivity and diffusion coefficients, properties which are important to understanding the oxidation mechanism. The lattice parameters found as a function of x are reproduced schematically as the curves in Figure 1. The points represent results of the present research as detailed below.

As is evident from this figure, these studies demonstrated that the composition (x) of the solid solutions cannot be determined satisfactorily from lattice parameter measurements alone. For this reason a combination scheme of quantitative X-ray diffraction intensity measurements to give the relative amounts of the phases present and colorimetric chemical analysis for the metals present was developed and applied to the air oxidation of the steels.[4] This was done in addition to the standard X-ray diffraction analysis.

Results

The essential results of the diffraction analysis and the combination diffraction-chemical analysis of the scales formed on the chromium steels listed in Table 1 under a variety of exposures to dry air and one atmosphere pressure of dry oxygen are shown in Tables 2 and 3 and Figure 2. Checks were made with other alloys of the 446, 440 and 430 types without significant variations.

The numbers given in the first row in each entry of Tables 2 and 3 are the mole fractions of the phases indicated in the second row by letter symbols. The rhombohedral structure types are indicated by R followed by a number giving the mole percent of Cr_2O_3 dissolved in αFe_2O_3; RO is αFe_2O_3 and R100 is Cr_2O_3. Spinel type oxides are shown by the symbol S preceded by LP or HP accordingly as the lattice parameter has the relatively low value of the Fe-Cr spinels or the high value of $MnCr_2O_4$. Wüstite type phases are shown by FeO preceded by L or H corresponding to relatively low or high values of the lattice parameter respectively. Additional phases which sometimes occur and their approximate mole proportions are added in parenthesis.

Data for alternative but less common scale structures are enclosed in square brackets. The results for the different layers of a scale are separated by

dotted lines: They are listed in order with the outermost layer at the top.

The additional data obtained for the chemically analyzed scales are listed in the order of the lattice parameters of the spinel and wüstite phases, the x value of Fe-Cr spinel, the Cr fraction of metal, and the total mg/cm² of metal in the layer. All lattice parameters are given in kX units for the reason that nearly all corresponding values quoted in the literature are actually in these units even when indicated in Angstrom units (1 kX unit = 1.00202 A unit).

It is evident from these data that the scale formed on chromium steels oxidized in air or oxygen is of two distinct types, A and B.

Type A Scale

Type A scale is associated with low rates of attack (low temperatures and high chrome alloys) and consists primarily of Cr_2O_3 together with an amount of αFe_2O_3 which is somewhat erratic but which in general decreases with an increase in the chromium content of the alloy and with a decrease in the oxygen partial pressure. This scale also may contain copious amounts of $MnCr_2O_4$ (HPS in Tables 2 and 3) when the steel contains sufficient manganese. Many auxiliary experiments involving both diffraction and chemical analyses have demonstrated that this phase has the composition $MnCr_2O_4$ very closely and that the amount of this phase, when it occurs, is roughly proportional to the Mn content of the alloy. It is not detectible at Mn levels below about 0.3 percent in a 26 percent Cr alloy; its occurrence is favored by low oxygen pressure, low temperatures, high chromium content of the alloy, and long oxidation times.

Because of the thinness of A scales, no positive determination of how the components are distributed in the scale has been possible. There are some indications, however, that both the Fe_2O_3 and the $MnCr_2O_4$ phases are external to the Cr_2O_3 phase. At sufficiently high temperatures and long times of oxidation there is a tendency for the ferric and chromic oxides to form dilute solid solutions, each in the other. In the two cases shown for AM-26 wherein the data are separated by dotted lines rather than dashed lines the upper data represent the scale as a whole and those below the line, the residue clinging to the metal. These data indicate that when both Cr_2O_3 and a ferric-chromic oxide solution are present, the former is in contact with the metal.

Some indication of the effect of minor constituents on the formation of A type scale was obtained from studies of the scale on a series of special Cr steels, in which the content of C, Mn, Si and N decreased in the order of samples S-2, S-3, S-4, S-5 (S-2 is AM-26). These samples were oxidized in air for 20 hours at 980 C with the results indicated in Table 4, using the same notation as in Tables 2 and 3.

It is evident not only that the $MnCr_2O_4$ phase disappears as the Mn content of the alloy decreases, as noted above, but also that a decrease in the minor constituents decreases the Fe_2O_3 relative to the Cr_2O_3 phase. Which minor component or combination of components is responsible is not known. This behavior is to be contrasted with the observation that repeated oxidations of a sample which is given a minimum of polishing between cycles results not only in a decrease in $MnCr_2O_4$ due to manganese depletion but also in an increase in Fe_2O_3 associated with the depletion of chromium.

Type B Scale

Type B scale, which occurs under high rate of attack conditions, consists of an oriented layer of αFe_2O_3 on the outer surface of one or more layers of the spinel type solid solutions, $FeFe_{(2-x)}Cr_xO_4$, (LPS in Tables 2 and 3). In the case of severe attack the spinel is accompanied by oxides of the FeO (wüstite) type in the inner layers. Exposure to air gives relatively more of the lower oxides than does oxygen exposure.

The particular orientation assumed by the Fe_2O_3 phase is understandable as a growth phenomenon. In the Fe_2O_3 structure the oxygen ions lie close packed in layers parallel to the (111) plane and these oxygen layers are interleaved with layers of the metal ions. Thus it is not surprising that the crystals should prefer to grow with the (111) plane parallel to the surface, for a whole layer of oxygen ions can be laid down, then a layer of metal ions, etc.

As the temperature of oxidation of a given alloy is increased, or as the chromium content of the alloy is decreased at a fixed temperature of oxidation, the data show that the scale type changes from A to B in accordance with the associated increase in attack. Over a narrow range of conditions the scale may contain elements of both types of scale. Within this range it is apparent that an initial scale of essentially the A type gradually changes to the B type as oxidation proceeds. The B type scale is itself very complex and requires more detailed consideration.

The Cr content of the spinel solution (x) in the innermost layer of the type B scale increases regularly with chromium content of the alloy and with temperature of oxidation (see Figure 2); the spinel existing in layers other than the innermost is essentially Fe_3O_4 ($x = 0$). The FeO type phases, if any, accompanying the spinels are of two kinds. That which occurs with Fe_3O_4 (LFeO in Tables 2 and 3) is the usual wüstite as found on pure iron, whereas that which coexists with the chromium bearing spinels (HFeO) has a higher lattice parameter and may be assumed to be a modified wüstite containing some chromium in solution. The higher parameter must be ascribed to a lower concentration of cation vacancies. This is reasonable in view of the observation made while working with the synthetic spinels that the equilibrium oxygen pressure of the modified wüstite is lower than that of ordinary wüstite. In these studies a good correlation was observed between high x values of the spinels, high lattice parameters of the wüstites and low oxygen pressures.

The spinel lattice parameters found in the analyzed layers are plotted in Figure 1. It is evident that these points confirm the general form of the curves obtained for the synthetic materials. Those spinels which occur without wüstite conform to the oxygen-rich curve or lie between it and the stoichiometric

curve; those which coexist with wüstite type phases tend to lie from 0.003 to 0.005 kX units above the stoichiometric ("metal rich") curve. This latter deviation is believed to be due to the presence of manganese in solution. It is estimated that less than 3 percent manganese (as metal) would be required and this is just below the limit of detectibility with the manganese analysis scheme used.

The composition and lattice parameter obtained for the spinel phase are mean values for the layer analyzed. However, a comparison with the synthetic spinels, Figure 1, and consideration of the range of uncertainty in the lattice parameter determinations (±0.003 kX) shows that in no case can an appreciable fraction of the layer be ferrous chromite (x = 2). Moreover, in the scale layers for which an x between about 1 and 1.5 is found by analysis, the range in x for the major portion of the layer cannot exceed about ±0.2. When a value of x well below 1 is observed the layer could contain two major fractions having x values near 0 and 1 respectively. In several instances of thick scales it was possible to obtain a scraping from the inside of the innermost layer (less than 10 percent of the layer); in these cases the spinel lines of the diffraction pattern were broader than normal and could include a range of x up to x = 2. Thus it is probable that ferrous chromite is in contact with the metal, but that with increasing distance into the scale x decreases rapidly to a value near that observed by analysis and thereafter has only a small gradient until the Fe_3O_4 layer is approached, whereupon it falls rapidly to zero. In a very thick scale this latter transition region may form a well defined ("middle") layer.

Figure 2 shows that in B type scale the chromium fraction of total metal in the inner layer or layers (corresponding to the FeO layer in the scale on pure iron) is about 1.8 times its value in the alloy, whereas the chromium fraction is essentially zero in the outer layer (corresponding to the Fe_3O_4 + Fe_2O_3 layer on iron) and exceeds that of the alloy by about 1 percent in the scale as a whole.

The overall picture of a fully developed B type scale is indicated schematically in Figure 3; the obvious effects which appear in Tables 2 and 3 resulting from the inability to cleanly separate layers have been omitted. In the case of less drastic attack or of higher oxygen pressures than are here visualized, the wüstite phases would be less prominent or missing.

A comparison of Tables 2 and 3 with attack rate data given in the literature as a function of alloy

TABLE 2—Structure of the Oxide Scales on Chromium Steels Oxidized in Dry Air

OXIDATION		SAMPLE											
Temperature (Degrees C)	Time (Hours)	AM-5			AM-13			AM-17			AM-26		
775	20	.40 LPS	.60 RO	....	.05 HPS	.50 RO	.45 R100	.10 HPS	.45 RO	.45 R100	.30 HPS	....	.70 R100
825	20	.30 LPS	.70 RO	....	.15 HPS	.45 RO	.40 R100	.30 HPS	....	.70 R100	.25 HPS	.10 RO	.65 R100
860	20	.36 LPS a = 8.376 x = 0.34	.18 RO 37 mg/cm²	.31 LFeO a = 4.283 .15 HFeO a = 4.31 6.0% Cr	....	....	....	....	....	....	....	....	....
900	5	.25 LPS	.40 RO*	.35 LFeO	.05 LPS	.40 RO	.55 R100	....	.40 RO	.60 R100	.40 HPS	....	.60 R100
		.35 LPS	....	.65 HFeO	....	....	....	[.30 HPS	....	.70 R100]	....	....	....
	20	.30 LPS	.40 RO*	.30 LFeO	.40 LPS	.60 RO*	....	.35 HPS	....	.65 R100	.40 HPS	.... (.10 RO)	.60 R100
		.15 LPS	.15 RO	.60 LFeO .10 HFeO	.50 LPS	.50 RO	....	[.40 LPS .80 LPS	.60 RO .20 RO	....]	....	....	....
		.20 LPS	....	.80 HFeO	....	....	....	....	....	....	....	....	....
	100	.40 LPS	.60 RO*	....	....	1.0 RO*	....	....	1.0 RO	....	.40 HPS	.... (.10 RO)	.60 R100
		.30 LPS	.60 LFeO	.10 HFeO	.30 LPS	.70 RO	....	....	1.0 R25	....	....	....	....
		.30 LPS	....	.70 HFeO	[.40 LPS	.60 RO	. ....]	[....	.10 RO	.90 R100]	....	....	....
		.25 LPS	....	.75 HFeO	.60 LPS	....	.40 R80]	....	....	....	....	....	....
925	20	.40 LPS a = 8.381 x = 0.0	.20 RO* 23 mg/cm²	.40 LFeO a = 4.282 0% Cr	.40 LPS a = 8.376 x = 0.0	.60 RO* 11 mg/cm²	.... 0.3% Cr	.34 LPS a = 8.380 x = 1.34	.66 RO 3.4 mg/cm²	.... 18.6% Cr	.40 HPS	.... (.10 RO)	.60 R100
		.26 LPS a = 8.373 x = 0.59	.05 RO 43 mg/cm²	.69 HFeO a = 4.29 9.2% Cr	.79 LPS a = 8.375 x = 1.1	.21 RO 16 mg/cm²	.... 24.5% Cr	[....	.65 RO	.35 R100]	....	....	....
		Total: 66 mg/cm² 6.1% Cr			Total: 27 mg/cm² 14.7% Cr			....	....	....	....	....	....

(Note: Table 2 Continued on Following Page.)

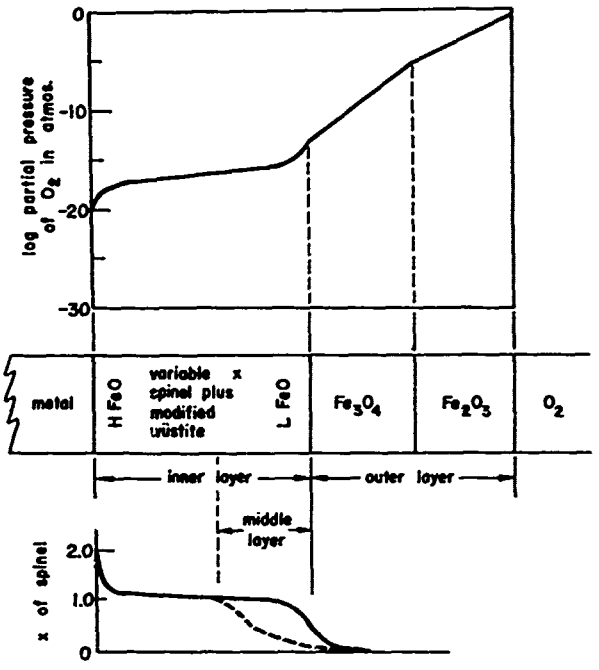

Figure 3—Schematic of fully developed B type scale.

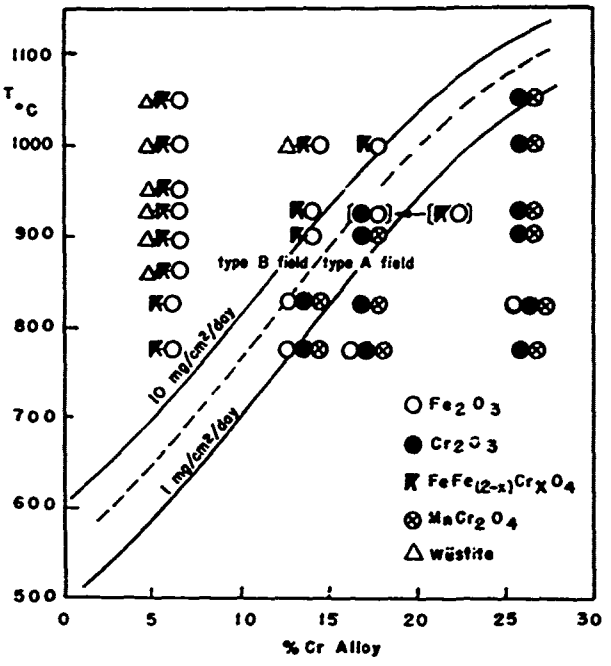

Figure 4—Oxides present and scale type on chromium steels after 10-20 hours of oxidation in air.

TABLE 2 (Continued)—Structure of the Oxide Scales on Chromium Steels Oxidized in Dry Air

OXIDATION		SAMPLE			
Temperature (Degrees C)	Time (Hours)	AM-5	AM-13	AM-17	AM-26
950	20	.40 LPS a=8.38 x=0.0 47 mg/cm² / .60 RO* / .... 0% Cr .28 LPS a=8.378 x=0.85 36 mg/cm² / .... / .72 HFeO a=4.30 14.5% Cr Total: 83 mg/cm² 6.3% Cr	....	....	....
	5	....	....	.... 1.0 RO .... / .65 R25 .35 R75	.20 HPS .... .60 R100
1000	10	.45 LPS a=8.380 x=0.0 58 mg/cm² / .40 RO* / .15 LFeO a=4.283 0.8% Cr .33 LPS a=8.380 x=0.05 84 mg/cm² / .... / .67 LFeO a=4.287 1.0% Cr .34 LPS a=8.385 x=1.08 60 mg/cm² / .... / .66 HFeO a=4.295 20.0% Cr Total: 202 mg/cm² 6.7% Cr	.40 LPS a=8.378 x=0 0 45 mg/cm² / .60 RO* / .... 0% Cr .40 LPS a=8.382 x=1.16 66 mg/cm² / .... / .60 HFeO a=4.296 24.6% Cr Total: 111 mg/cm² 14.7% Cr	.27 LPS a=8.376 x=1.52 22 mg/cm² / .73 RO* / .... 18.2% Cr	.40 HPS .... .60 R100 .... 3.4 mg/cm² ....
1050	20	.30 LPS / .45 RO* / .25 LFeO .40 LPS / .... / .60 LFeO .40 LPS / .... / .60 HFeO	....	....	.30 HPS .... (.10 RO) .70 R100

Note: Numbers in the first row are the mole fractions of the phases indicated in the second row, as follows:
1. Rn—Rhombohedral phase; n mole percent of Cr_2O_3 in a Fe_2O_3 solid solution. RO—Fe_2O_3; RO*—a Fe_2O_3 oriented with (111) plane parallel to surface R100—Cr_2O_3.
2. HPS—Spinel phase. $MnCr_2O_4$; lattice parameter between 8.435 and 8.420 kX. LPS—Spinel phase. $FeFe_{(2-x)}Cr_xO_4$; lattice parameter between 8.387 and 8.373 kX.
3. LFeO—Cubic structure of FeO (wustite) with lattice parameter between 4.287 and 4.282 kX. HFeO—Ditto with parameter between 4.310 and 4.290 kX. (1 kX unit = 1.00202A unit).

Additional phases sometimes present and their approximate mole proportions are given in parenthesis. Alternative scale structures are enclosed in square brackets.

Data for different layers are listed in order with the outermost layer at the top.

For certain scales which were analyzed chemically, additional information is listed in the following order: Lattice parameters in kX of spinel and FeO phases; x value of $FeFe_{(2-x)}Cr_xO_4$ spinel; Cr fraction of metal in the layer in weight percent; mg/cm² of metal in the layer.

composition and time and temperature of oxidation[1,5,6,7,8] indicates that there is a very pronounced correlation between the transition from A to B scales and an attack rate of approximately 10 mg/cm² of metal loss per day. This relationship is illustrated in Figure 4 for the 10 to 20 hour oxidations in air. The data for one atmosphere pressure of oxygen are similar with more αFe_2O_3 and less wüstite present. Such comparisons clearly show that presence of Cr_2O_3 is the essential element of a satisfactory scale. When a B type scale is formed the attack is much heavier: it is, in fact, excessive since the maximum acceptable rate in ordinary practice is essentially the same as the critical value observed for the A to B transition.

Discussion

Several of the results summarized in Tables 2 and 3 and Figure 2 already are contained in the literature. The general correlation of a decreasing attack rate with an increase in the chromium content of the alloy is well known.[1,5,6,7,8] Much of the additional information which is available is in the form of isolated facts which, without the interpretation now possible from the more systematic investigations, often appear to be inconsistent or even contradictory.

The confusion arises primarily from a lack of appreciation of the fact that two distinct types of scales occur. This fact was clearly noted by Scheil and Kiwit[5] in the case of Al-Cr-Fe alloys and it was implicit in their results for the Cr-Fe alloys but was perhaps too little emphasized. Although Scheil and Schulz[6] correctly described the principal components of A type scale as Cr_2O_3 or $Cr_2O_3 + Fe_2O_3$, they incompletely represented B scale as Fe_2O_3 on their charts. This interpretation was not explicitly corrected by Scheil and Kiwit who gave chemical analyses of inner and outer layers of B scale similar to those shown in Figure 2. With the more nearly complete separation of inner and outer layers obtained, a more regular variation of chromium in the inner layer was found in the present work than was found by the above authors. Practically no chromium was found in the outer layer (i.e., the layer corresponding to Fe_2O_3 and Fe_3O_4 layers on pure iron).

Rickett and Wood[7] found the scale on chromium steels occurs in layers which decreased in number as the Cr content of the alloy increased. The outer layers were made up of $(Fe,Cr)_2O_3$ and the inner of $(Fe,Cr)_3O_4$. But without further specification of the composition of these phases and how they depend

TABLE 3

Structure of Oxide Scales on Chromium Steels Oxidized in One Atmosphere of Dry Oxygen

Oxidation		SAMPLE											
Temp. (Degrees C)	Time (Hours)	AM-5			AM-13			AM-17			AM-26		
700	20	.10 LPS	.90 RO	....	....	.45 RO	.55 R100	....	.50 RO	.50 R100	....	.35 RO	.65 R100
775	20	.20 LPS	.80 RO*	....	....	.65 RO	.35 R100	....	.45 RO	.55 R100	.20 HPS	.20 RO	.60 R100
825	2	....	.90 RO	.10 R100	....	.70 RO	.30 R100	....	.65 RO	.35 R100	....	.35 RO	.65 R100
	20	.20 LPS	.80 RO	....	....	.70 RO	.30 R100	....	.70 RO	.30 R100	.20 HPS	.20 RO	.60 R100
		.50 LPS	.45 RO	.05 LFeO	....	....	....	....	....	....	....	....	....
900	½	.40 LPS	.55 RO	.05 R100	.30 LPS	.50 RO	.20 R100	.20 LPS	.50 RO	.30 R100	....	.35 RO	.65 R100
	5	.40 LPS	.60 RO*	....	.20 LPS	.60 RO	.20 R100	.15 LPS	.60 RO	.25 R100	.15 HPS	.30 RO	.55 R100
		.25 LPS	.15 RO	.60 HFeO	....	....	....	....	....	....	....	....	.. ...
	20	.40 LPS	.60 RO*	....	.20 LPS	.70 RO*	.30 R100	.20 LPS	.70 RO	.30 R100	.15 HPS	.55 RO (.30-R25)	.30 R100
		.30 LPS	.20 RO	.50 LFeO	....	....	....	....	....	....	....	....	....
		.40 LPS	....	.60 HFeO	....	....	....	....	....	....	....	....	....
	100	....	1.0 RO*	....	....	1.0 RO*	....	....	1.0 RO	....	.20 HPS	.50 RO	.30 R75
		.40 LPS	.60 RO	....	.30 LPS	.40 RO (.30-R75)	.30 R100	....	.60 RO	.40 R25	.25 HPS	.40 RO (.60-R100)	.35 R75
		.80 LPS	....	.20 LFeO	....	....	....	....	....	....	....	....	....
		.35 LPS	....	.65 HFeO	....	....	....	....	....	....	....	....	....
950	20	.30 LPS	.70 RO*	....	.30 LPS	.70 RO*	....	.30 LPS	.70 RO	....	.40 HPS	....	.60 R100
		.45 LPS	.25 R25	.30 HFeO	[	.70 RO	.30 R100]	[	1.0 R-25-50	]	....	....	....
	100	....	....	....	....	....	....	....	....	....	.50 HPS	(.50) (R65)	.50 R100
		....	....	....	....	....	....	....	....	....	.40 HPS	....	.60 R100
1000	½	.40 LPS	.60 RO	....	.25 LPS	.55 RO	.20 R100	.20 LPS	.50 RO	.30 R100	....	....	1.0 R100
	10	.50 LPS	.50 RO*	....	.40 LPS	.60 RO*	....	.40 LPS	.60 RO*	....	.40 HPS	....	.60 R100
		.50 LPS	.25 RO	.25 LFeO	.50 LPS	.50 RO	....	.75 LPS	.25 RO	....	....	....	....
		.50 LPS	.20 RO	.30 HFeO	....	....	....	....	....	....	....	....	....
1100	10	....	....	....	....	1.0 RO*	....	....	1.0 RO*	....	.40 HPS	.05 R25	.55 R100
		....	....	....	....	.60 RO	.40 R75	....	.50 RO	.50 R20	....	....	....
		....	....	....	.50 LPS	.50 RO	....	....	....	....	....	....	....
1160	5	....	....	....	....	....	....	....	1.0 RO*	....	.20 HPS	.80 R20	....
		....	....	....	....	....	....	....	.65 RO	.35 R15	.25 HPS	.60 R20	.15 R85

Note: Numbers in the first row are the mole fractions of the phases indicated in the second row, as follows:

1. Rn—Rhombohedral phase; n mole percent of Cr_2O_3 in αFe_2O_3 solid solution. RO—Fe_2O_3: RO*—αFe_2O_3 oriented with (111) plane parallel to surface. R100—Cr_2O_3.
2. HPS—Spinel phase. $MnCr_2O_4$; lattice parameter between 8.435 and 8.420 kX. LPS—Spinel phase. $FeFe_{(2-x)}Cr_xO_4$; lattice parameter between 8.387 and 8.373 kX.
3. LFeO—Cubic structure of FeO (wustite) with lattice parameter between 4.287 and 4.282 kX. HFeO—Ditto with parameter between 4.310 and 4.290 kX. (1 kX unit = 1.00202A unit).

Additional phases sometimes present and their approximate mole proportions are given in parenthesis. Alternative scale structures are enclosed in square brackets.

Data for different layers are listed in order with the outermost layer at the top.

upon oxidation conditions these results do not give a description which is amenable to further comparison.

McCullough, Fontana and Beck[8] have observed the onset of a rapid increase in the oxidation rate of chromium (and nickel-chromium) steels after an initial low rate and have ascribed this change to a transition from a protective ferrous chromite scale to a less protective hematite scale. This interpretation is not supported by their chemical analyses which give a Cr to Fe ratio varying between four and nine in the initial scale, then decreasing to less than unity. Thus the initial scale must have contained a large fraction of Cr_2O_3. The analyses are consistent with a change from an initial A type to a B type scale in accordance with similar transitions shown in Tables 2 and 3 (e.g., for AM-17 at 900 C).

Moreau[9] gives a brief description of a B type scale which, although similar from an overall point of view, differs from the authors' findings in several important respects. A significant thickness of an $FeCr_2O_4$ + FeO inner layer rather than a thin transition layer is postulated. The spinel x value is treated as remaining at 2 over this innermost layer, then falling rapidly to zero. Thus no dependence of x on the composition of the alloy is admitted. No possibility is provided for the existence of FeO in either the innermost layer or in the middle layer. Since no specific indication is given of the exposure conditions for each alloy it is not made obvious that this description could apply only to the most extreme attack; no mention is made of the profound changes which occur under less severe conditions.

The latter limitation applies to a lesser degree to the very complete micrographic examination of B type scales given by Portevin, Prétet and Jolivet[10] since they imply in their conclusions that for higher chrome alloys the scale character changes. It is clear that the separation of "A" and "B" layers observed by them corresponds to the authors' division into inner and outer layers. Their A_1 component next to the metal is interpreted as the thin transition layer from $x = 2$ to the analyzed value, A_2 as the region of nearly constant x and A_3 as the transition region to $x = 0$.

Cohen and Caplan[11] give a complete description of an A type scale formed in several hundred hours on an alloy similar to AM-26. The interpretation is complicated by the occurrence of a duplex structure, presumably caused by blistering. Although it is not completely evident from the publication, private communication has established that the phases present were the same as those obtained by the authors, including $MnCr_2O_4$, with the addition of α crystobalite. The crystalline silica probably is related to an amorphous film which was observed beneath the scale in the authors' much shorter oxidations.

In nearly all cases of true A scale formation the scale was easily removed after cooling. In this event a temper color film was observed on the metal, and for the longer oxidations this was accompanied by a layer having a white or frosty appearance. Electron micrographs of the exposed surface by replica and by transmission through stripped films showed that the latter material had a rough surface and was nearly opaque to 50 kv electrons ($\simeq 10^{-5}$ cm thick). It was located external to a thin film which was shown by electron diffraction to consist of oxides of iron and chromium.

X-ray diffraction revealed no diffraction except for two diffuse halos and those very weak patterns which could be ascribed to the thin film. Thus the massive material was amorphous. No successful chemical analysis of this material has been possible but microanalyses[12] of the removed scale have shown several percent of silicon. It is tentatively assumed therefore that the material is an amorphous silica or a silicate. A more detailed description of these layers occurring under A type scales and of the evidence which strongly suggests that they exist at temperature, rather than that they form during cooling, will be published elsewhere.

Oxidation Mechanisms

Equilibrium Diagrams

From these experiments it is now possible to give a rather detailed description of the composition and disposition of the various oxide phases occurring in the scale as a function of alloy composition, of time and temperature of oxidation, and of oxygen pressure. One is in position, therefore, to propose tentative oxidation mechanisms for test by further experiments. Essential for this purpose is a knowledge of the basic properties of the oxide phases. Since some information is available concerning the other pertinent oxides, investigations are being made of the structure and electrical conductivity of the Fe-Cr spinels.

One of the most useful pieces of information would be a complete knowledge of the Fe-Cr-O phase diagram: some facts concerning these equilibria have been accumulated in studies of the formation and of the oxidation and reduction of the Fe-Cr spinels.[3] The simplest form of phase diagram which is in agreement with the observations is represented schematically by the full lines in Figure 5 for low temperatures where the metals are completely miscible. The single phase homogeneity ranges have been exaggerated for clarity. "Phases" will refer here to solid phases. The single phase solutions of the spinels and of the ferric-chromic oxides are well established. The two phase regions connecting the spinels to the

TABLE 4—Effect of Minor Constituents of the Alloy on the Structure of A Type Scale

Alloy	S-2 26.31 Cr				S-3 27.88 Cr				S-4 26.01 Cr				S-5 25.47 Cr			
	C	Mn	Si	N	C	Mn	Si	N	C	Mn	Si	N	C	Mn	Si	N
	0.14	0.68	0.74	0.115	0.05	0.38	0.54	....	0.022	0.12	0.16	0.016	0.009	0.01	0.12	0.018
Scale	.30	.10	.60	....	.15	.10	.75	....	....	.05	.95	....	....	.05	.95	....
	HPS	RO	R100	....	HPS	RO	R100	....	....	RO	R100	....	....	RO	R100	....

ferric-chromic solutions and to the modified wüstites were observed in working with the synthetic spinels. It was observed qualitatively that the corresponding equilibrium oxygen pressures decrease rapidly as the chromium content of the phases increases. It is assumed that this trend continues from composition d to pure Cr_2O_3.

It is to be emphasized that the arrangement shown, particularly with regard to the region a, b, c, d, e, is tentative. No necessity for the assumption of a pseudo-binary between oxygen-rich Cr and Fe has been visualized.[5,13,14] Even so, other arrangements are possible. At an alloy composition such as e, a three phase region c, d, e, might be interposed between a pseudo-binary, Cr-Cr_2O_3, and a two phase region extending from alloys a-e to a small range near $FeCr_2O_4$ (Case 2).

In view of the discussion below, a more attractive variation of this last arrangement would be obtained if point e were near point a, leaving the diagram as drawn except for a narrow pseudo-binary between a and c, as indicated by the pair of dashed lines (Case 3). At higher temperatures the miscibility gap of the alloys can be taken into account in Case 1 and Case 3 by dividing the upper two phase region into two by a three phase region based on the $\alpha + \delta$ alloy range f-g and terminating near d, as indicated by the dotted lines. The two other possibilities for which this region would terminate at b or c would predict the wrong type of scale on alloys near f, according to the considerations to follow.

Case 1 requires a fixed composition for $FeCr_2O_4$ whereas 2 and 3 require a range of homogeneity. The spinel lattice parameter measurements[3] indicate a very small range but cannot eliminate the possibility of a fixed composition (not necessarily the stoichiometric one).

Equilibrium diagrams have been used to interpret the oxides formed on binary alloys. Scheil and Kiwit[5] and Scheil[12] have considered that the oxide which will be formed at the metal is the one having the largest heat of formation. They treated the single phase regions as having fixed compositions, thus the ranges of composition necessary for the formation of scale layers in which diffusion can occur were not included. Rhines[14] has taken this into account and has applied these ideas with considerable success to the external and internal oxidation (subscale) of copper alloys. In particular he shows that it is not necessarily the most stable oxide which forms on the metal (e.g., according to Figure 5, modified wüstite would form on an alloy of Cr content less than composition a, although Cr_2O_3 is more stable in the usual sense).

Wagner Theory

Considerations based on equilibrium diagrams can form only a starting point for interpretation since they tell only what phases should be present at equilibrium and for known compositions. The actual situation is a dynamic one and the amount of the components present in a layer depends in a very complex way on reaction rates at interfaces and on diffusion rates within the various layers and within the

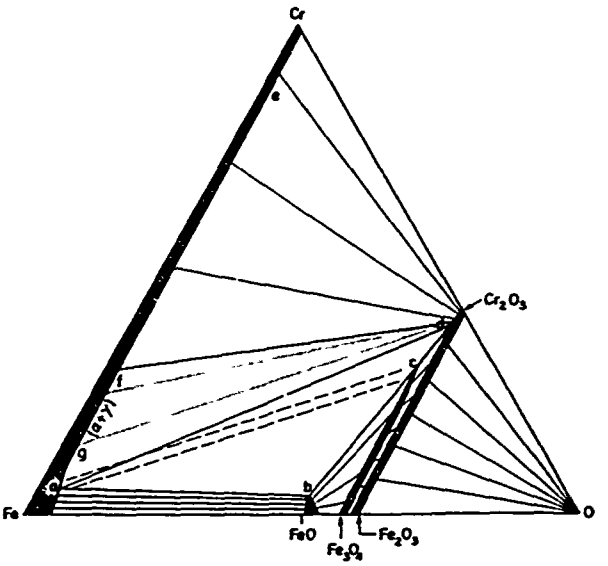

Figure 5—Schematic Fe-Cr-O constitution diagram.

alloy. Dunn[15] has treated the problem taking into account some of the effects of differential diffusion within a binary alloy and the oxides formed on it. The more quantitative treatment of Wagner[16] is more fruitful, however, for the present considerations.

Under the simplifying assumptions of ideal solution behavior of the binary alloy, no mutual solubility of the oxides and approximate equilibrium at the metal-oxide interface, Wagner has investigated the conditions under which a single oxide of one metal or the other, or mixtures of the two oxides, will be formed. The assumptions made are not completely fulfilled in the present instance, but the qualitative features of the theory are informative.

Equilibrium of either component of the alloy with its corresponding oxide of dissociation pressure π, relative to the pure metal, requires that $N^m p = \pi$, where N is the mole fraction at the interface of that component, p is the equilibrium oxygen pressure at the interface and m is a positive number (4/3 for Cr-Cr_2O_3 and 2 for Fe-FeO). Since $N_{Fe} = 1 - N_{Cr}$, for a large N_{Cr} the equilibrium pressure for Cr would be less than that for Fe and only Cr_2O_3 would be formed; for a large N_{Fe} the reverse is true and only wüstite would be stable.

At some critical N_{Cr} the equilibrium pressures would become equal and both oxides could exist (in the absence of oxide solubilities and compound formation). Because $\pi(Cr_2O_3)$ is several orders of magnitude lower than $\pi(FeO)$[17] the critical composition would be at a very low mole fraction of Cr. The existence of ranges of composition of the oxides as envisaged in Figure 5 modifies this picture somewhat. If the dissociation pressure of the chromic oxides increases on going toward d and that of the modified wüstites decreases toward b, as assumed, the critical mole fraction of Cr would be increased to some value represented by a.

This mechanism then provides for type A and B scales. If the concentration of chromium is above point a, essentially pure Cr_2O_3 or A type scale would

be formed, whereas if it is below only modified wüstite should be present. In either of these situations, however, it is clear that surface depletion of the oxidizing component would occur, tending to bring the surface concentration to a. At this concentration either modified wüstite and approximate Cr_2O_3 of composition d would form (Case 1), giving the essentials of a B type scale when they react to the spinel and excess wüstite, or $FeCr_2O_4$ would form directly (Case 3). It follows from the limited rate of diffusion of chromium in the alloy that if an A type scale is to be formed the bulk concentration must be considerably larger than a. Similarly, if only wüstite is to be formed, the bulk concentration must be considerably smaller than a (actually very near pure Fe). For alloys between these compositions a B type scale will be produced.

Application of the Wagner concepts and use of the phase diagram leads to the conclusion that under conditions appropriate to B scale formation either wüstite and Cr_2O_3, or $FeCr_2O_4$ should form at the interface. But such considerations alone cannot tell how much of the metal components will be oxidized nor how they will be distributed through the scale.

In Figure 2 it is shown that for B scale the overall composition is the same as that of the alloy except for about 1 percent excess of chromium. This is understandable when it is realized that the total thickness of metal which is oxidized in an ordinary observational period is large compared with the depth from which an appreciable amount of Cr can diffuse. Thus in B scale formation the metal components must enter the scale in nearly the alloy proportion, with a slight excess of chromium which comes from setting up the chromium gradient. Since with any practical alloy there will always be more than enough iron present, all Cr_2O_3 (Case 1) should be reacted to spinel at the interface or immediately adjacent to it. Cr_2O_3 should not be found in B scale except possibly as a subscale layer on and within the metal.

The proportions of the metals in the scale at any point will not in general be the same as in the alloy since their rate of transport through the oxide is not the same. Not only do possible differences of diffusion coefficient come into play but a whole series of displacement reactions is active within the spinel layer as well as interface reactions at the boundaries of the layers. Chromium can displace iron from any of the spinels. Since the equilibrium pressure for high chrome spinels is lower than for low chrome spinels, under the conditions of an oxygen pressure gradient a tendency always will exist for the high chrome spinels to segregate at the inside of the inner scale and a gradient of spinel composition (x) will be obtained (Figure 3).

If the rate of decrease of x is sufficiently large compared with the rise in oxygen pressure corresponding to increasing distances from the metal-oxide interface, the spinels will come to their metal-rich state and be accompanied by the corresponding modified wüstite. It might be thought that this condition would lead to a reduction in attack rate since the gradient of cation vacancies in the spinels would then be small or essentially zero if the metal rich state corresponds to the stoichiometric composition. The high diffusion through the wüstite would compensate, however, for this decrease. Even in this case there might be some transport of chromium through the spinel phase by displacement reactions since local equilibrium with the wüstite might not exist, in view of the fact that as the scale thickens the effective oxygen pressure at any point decreases and spinels of higher x become stable.

Outward from the point at which x becomes zero the processes of scale formation are similar to those which occur in the scaling of pure iron, resulting in the formation of Fe_3O_4 and Fe_2O_3 outer layers.

Moreau's Mechanism

This mechanism is in strong contrast with that proposed by Moreau.[9] Since he postulates an appreciably thick layer of stoichiometric $FeCr_2O_4$ in which diffusion cannot occur and further assumes that the accompanying FeO cannot diffuse trivalent ions, he is brought to the conclusion that all chromium is reacted at the interface with oxygen which diffuses inward through the layer. Thus the $FeCr_2O_4$ components grow at the inside boundary of the layer and dissolve in the Fe_3O_4 layer at the outside boundary to form spinels with x less than 2. Extension of the latter reasoning leads the authors to believe that an appreciable thickness of $FeCr_2O_4$ would not form initially and that the gradient in x would begin at the metal-oxide interface as observations indicate.

It is well known that wüstite contains Fe^{3+} ions associated with the large metal deficiency which always exists. The vacancy concentration may be as high as 10 percent of the cation sites[18,19] and more than 20 percent of the cations may be trivalent. There is no objection, therefore, to the assumption that Cr^{3+} can disolve in and diffuse through the "modified" wüstite phase when it is present. As already has been pointed out, there is good evidence that the modified wüstites have lower concentrations of cation vacancies than does ordinary wüstite and would, therefore, be expected to have smaller diffusion coefficients. This may be the primary reason that the B type scale, although less protective than A scale, is more protective than the scale on pure iron.

In the alternate case that no wüstite phase is observed, which situation is not compatible with the hypothesis of Moreau, the spinels are cation deficient and can certainly diffuse both iron and chromium ions. Furthermore, if the rate of loss of chromium were determined by the rate of inward diffusion of oxygen, it would seem difficult to account for the near identity of the chromium to iron proportions in scale and alloy for a wide range of conditions as shown in Tables 2 and 3 and Figure 2. This difficulty is particularly great if consideration is given to the great disparity in the diffusion rates of oxygen and metal in Fe_3O_4 and in FeO observed by Himmel, Mehl and Birchenall.[18]

Growth Law

Under the assumption that the scale follows the parabolic growth law and that the interdiffusion co-

efficient in the alloy is independent of concentration, the Wagner theory shows that the critical bulk concentration of chromium which would differentiate A from B scale is an increasing function of the ratio of the parabolic rate constant, K, to the interdiffusion coefficient in the alloy, D.

It is known that the scale on chromium steels does not grow according to the parabolic law $y^2 = Kt$, but in a manner[7,8] more nearly $y^n = K't$ where n is less than 2. In terms of the parabolic law, K increases with time of oxidation, and therefore the critical bulk concentration increases with time. Conversely then, the A type scale which may be formed initially on a given alloy must eventually change to the B type. Several instances of this change with time are evident in Tables 2 and 3. Of course, if the chromium content of the alloy is sufficiently high (e.g., 26 percent) the change may not be observed within the usual period of measurement.

Another feature of the theory is that of two alloys which oxidize to give Cr_2O_3, the one of lower chromium concentration should have a lower rate of metal loss. A lower N_{Cr} requires a higher equilibrium oxygen pressure, p, at the interface and this in turn entails a smaller concentration gradient of cation vacancies in the oxide lattice which results in a lower transport of chromium. The obvious deviation from this prediction of the idealized theory is probably associated with another equally obvious deviation: namely, the presence of Fe_2O_3 in A type scale. An analogous situation in the oxidation of Ni-Cu alloys has been considered by Wagner and the explanation of the present case is probably similar.

It is true that under the conditions assumed for the production of A type scale no oxide should be formed except pseudo Cr_2O_3 (in the case of a pure binary alloy), but Fe can oxidize in the initial stage before a protective layer is formed and subsequently at any local failure of the scale due to cracking or spalling. Non-equilibrium conditions might also be expected during α-δ transitions in the alloy. Furthermore, the balance between A and B scale formation is rather delicate and any local fluctuation in N_{Cr} may permit formation of iron oxides. Fluctuations of this nature might be present as initial inhomogeneities in the alloy or they would be produced during oxidation by any inclusion such as a carbide which would locally suppress diffusion of chromium to the alloy surface.

Whatever the cause of the formation of Fe_2O_3 in the scale, it is clear that the distribution of this phase must be rather heterogeneous. Otherwise ferric-chromic oxide solid solutions would be observed rather than separate phases, since intimate mixtures of these oxides will sinter completely to the solution in 10 to 20 hours at 950 C. Actually, significant amounts of solution are observed only at considerably higher temperatures or longer times.

Formation of iron oxide inclusions with the Cr_2O_3 will, of course, increase the rate of attack since these oxides are less protective. Tables 2 and 3 show that the amount of the Fe_2O_3 phase present in A type scale decreases as the chromium content of the alloy increases. This probably accounts for the corresponding decrease in attack rate. It also is noted that the amount of Fe_2O_3 for a given alloy and temperature of oxidation tends to increase with time. On the same basis as above, the associated decrease in protective quality may account for the deviation from the parabolic law and the eventual conversion to a B type scale, as discussed previously.

Other possible sources of deviation from the parabolic law may be associated with the presence of the thin film-like layer at the metal-scale interface which was described above, or with the presence of $MnCr_2O_4$ in the scale. No positive indications of the beneficial or detrimental effects of this phase have been observed.

Behavior of Manganese

The behavior of Mn in A type scale might be treated to a rough approximation by considering Fe to act as an inert solvent for the Mn and Cr. The mole fraction of each solute is nearly independent of changes in the other and the effective oxygen pressure at the metal-oxide interface is determined essentially by the N_{Cr} corresponding to equilibrium with the Cr_2O_3.

For simultaneous formation of the oxides at the same equilibrium pressure a critical chromium concentration will be required such that $N^\circ_{Cr} = \pi(Cr_2O_3)/\pi(MnO)^{2/3}(N_{Mn})^{2/3}$, neglecting solubilities of the oxides. Since the ratio of dissociation pressures is large, the N°_{Cr} will be much larger than the existing N_{Mn}. Three cases are to be distinguished. If N_{Cr} at the interface is larger than the critical value, the equilibrium pressure will be too low for the formation of MnO and no manganese should occur in the scale except to the limit of its solubility in Cr_2O_3 (or possibly in the metastable iron oxides present). When N_{Cr} is equal to N°_{Cr} both oxides should form. The fact that no MnO but only $MnCr_2O_4$ is observed must mean that conditions for reaction to the latter compound are reached at a position very near the interface or, in view of the effect of oxide solubilities and the unknown Mn-Cr-O phase diagram, direct formation should perhaps be considered instead of MnO. In either instance the excess Cr_2O_3 would effectively act as a sink for Mn and the amount of the latter in the scale would be controlled by its rate of diffusion in the metal.

The third case comes about when N_{Cr} becomes considerably less than the critical value, either due to a low bulk value or to the increased surface depletion associated with an increased attack rate. The pressure at the interface is then above that required for oxidation and MnO (or $MnCr_2O_4$) can be expected to occur as a subscale. This is probably the reason for the disappearance of the $MnCr_2O_4$ from the A scale on the lower chrome alloys in oxygen.

Unfortunately, a satisfactory quantitative check of these speculations cannot be made because of uncertainty in the value of $\pi(MnO)$. From the data available,[17,20] the ratio of dissociation pressures may be calculated in the temperature range of 800 to 1000 C as approximately 3×10^2 or 10^4. These values

correspond to an N°_{Cr} for 0.5 percent N_{Mn} of about 2 percent and 35 percent, respectively. Reasonable estimates of the value required by the experimental observations lie in this range.

Considerations similar to the above should apply also to Si, but since the dissociation pressure of SiO_2 is even lower than that of MnO it is expected to occur only in a sub-scale. If either the Mn or Si were present in sufficient amount, however, it could be expected to oxidize exclusively in a way analogous to that already discussed with respect to Cr and Fe.

Acknowledgments

This research was conducted under the auspices of Project Squid, jointly sponsored by the U. S. Office of Naval Research and the Office of Air Research under contract N6-ori-104, and of the U. S. Office of Naval Research under contract N7-onr-39419.

The authors are happy to thank the following individuals and firms for provision of the alloys with which this research was carried out: S. A. Lapham, American Rolling Mills; J. K. Stanley, Standard Oil Company of Indiana; W. O. Binder, H. R. Spendelow, Jr., and A. B. Kinzel, Union Carbide and Carbon Company; J. H. Gillan, Joseph T. Ryerson and Son, Inc. They are also greatly indebted to E. M. Mahla, N. A. Nielsen and T. N. Rhodin of the DuPont de Nemours Research Laboratory for their cooperation with certain chemical analyses, and to M. Cohen and D. Caplan of the Division of Applied Chemistry, National Research Council of Canada, for the privilege of discussing their oxidation data.

References

1. H. H. Uhlig The Corrosion Handbook. The Electrochemical Society, New York, 1948, p. 644.
2. P. E. Wretblad. *Z. anorg. u. allgem. Chem*, **189**, 331 (1930).
3. H. J. Yearian, J. M. Kortright and R. H. Langenheim. *J. Chem. Phys.*, **22**, 1196 (1954).
4. T. A. Longo. M. S. Thesis, Purdue University, 1953.
5. E. Scheil and K. Kiwit. *Arch. Eisenhuttenwesen*, **9**, 405 (1936).
6. E. Scheil and E. Schulz. *Arch. Eisenhuttenwesen*, **6**, 155 (1932).
7. R. L. Rickett and W. P. Wood. *Trans Am. Soc. Steel Treat.*, **22**, 347 (1934); K. Heindlehofer and P. M. Larson. *Ibid.*, **21**, 865 (1933).
8. H. M. McCullough, M. G. Fontana and F. H. Beck. A.S.M. (1950), Preprint No. 4.
9. J. Moreau. *Compt. rend.* **236**, 85 (1953).
10. A. Portevin, E. Prétet and H. Jolivet. *J. Iron and Steel Inst.*, **130**, 219 (1934).
11. M. Cohen and D. Caplan. *Jour. of Metals*, **4**, 1057 (1952).
12. The authors are indebted to E. M. Mahla, N. A. Nielsen and T. N. Rhodin of the duPont de Nemours Research Laboratory for these analyses.
13. E. Scheil. *Zeit. Metallkde.*, **29**, 209 (1937).
14. F. N. Rhines. *Trans. A.I.M.E.*, **137**, 246 (1940).
15. J. S. Dunn. *Jour. Inst. Met.*, **46**, 25 (1931).
16. C. Wagner. *Jour. Electrochem. Soc.*, **99**, 369 (1952).
17. L. S. Darken and R. W. Gurry. Physical Chemistry of Metals. McGraw-Hill, N. Y., 1953, page 349.
18. L. Himmel, R. F. Mehl and C. E. Birchenall. *Jour. of Metals*, **5**, 827 (1953).
19. E. R. Jette and F. Foote. *Jour. Chem. Phys.*, **1**, 29 (1933).
20. M. deKay Thompson. The Total and Free Energies of Formation of the Oxides of Thirty-Two Metals, The Electrochemical Society, N. Y. 1942.